Attitude Stability of an Orbiting Gyrostat in Conical Equilibrium

P.C. Hughes*
University of Toronto, Ontario, Canada

Satellites designed with large offset-dish reflectors create interest in configurations whose principal axes are not aligned with the orbiting axes. The resulting gravity-gradient torque about the roll axis can be balanced by the reaction torque from a body-fixed wheel or rotor parallel to the yaw axis. This leads to a consideration of the stability of a new class or orbiting gyrostats. It is shown in this paper that most such cases are unstable with respect to attitude perturbations. However, by adding a pitch wheel (which does not affect the equilibrium itself), it is demonstrated that stability can usually be achieved.

Introduction

A "RIGID GYROSTAT" is a rigid body $\mathfrak{R}$ with an associated rigid spinning wheel $\mathfrak{W}$ whose axis is fixed in $\mathfrak{R}$. In practice, $\mathfrak{W}$ may be either *internal* to $\mathfrak{R}$, as in a bias-momentum satellite, or *external* to $\mathfrak{R}$, as in a dual-spin design. We shall assume here that the gyrostat $\mathfrak{R}+\mathfrak{W}$ is in a circular orbit about an inverse-square gravitational primary. The attitude motion equations for the gyrostat are

$$\boldsymbol{I}\dot{\boldsymbol{\omega}}+\boldsymbol{\omega}^{\times}(\boldsymbol{I}\boldsymbol{\omega}+\boldsymbol{h}_s)=3\omega_c^2\boldsymbol{c}_3^{\times}\boldsymbol{I}\boldsymbol{c}_3 \tag{1}$$

where $\boldsymbol{I}$ is the inertia matrix for $\mathfrak{R}+\mathfrak{W}$, $\boldsymbol{\omega}$ is the absolute angular velocity of $\mathfrak{R}$, $\boldsymbol{h}_s$ is the angular momentum of $\mathfrak{W}$ relative to $\mathfrak{R}$, ω_c is the "orbital frequency," and $\boldsymbol{c}_3$ is the unit vector in the vertically down direction (see Fig. 1). All components in Eq. (1) are expressed in the centroidal body-fixed frame $\mathfrak{F}_p$ aligned with the principal axes of $\mathfrak{R}+\mathfrak{W}$. [The notation $(\ )^{\times}$ implies the 3×3 skew-symmetric cross-product matrix associated with the 3×1 column $(\ )$.]

Roberson and Hooker[1] were among the first to ask the following question: Under what conditions can a relative equilibrium exist in which the gyrostat remains fixed with respect to an orbiting frame $\mathfrak{F}_c$? ($\mathfrak{F}_c$ is shown in Fig. 1.) To state their answer precisely, a few new symbols are essential. Let

$$h_c \triangleq I_2\omega_c \tag{2}$$

denote the basic angular momentum of $\mathfrak{R}+\mathfrak{W}$ in orbit, with $\mathfrak{W}$ not spinning (i.e., with $\boldsymbol{h}_s=\boldsymbol{0}$). Next, let

$$\hat{\boldsymbol{h}}_s \triangleq \boldsymbol{h}_s/h_c \tag{3}$$

be the dimensionless vector that measures the relative angular momentum of $\mathfrak{W}$, in h_c units. Last, we denote the components of $\hat{\boldsymbol{h}}_s$ in $\mathfrak{F}_c$ by $\hat{h}_{si}$, $i=1, 2, 3$:

$$\hat{h}_{si} \triangleq \boldsymbol{c}_i^T\hat{\boldsymbol{h}}_s \tag{4}$$

where $\boldsymbol{c}_i$ are the unit vectors along the roll, pitch, and yaw axes (Fig. 1) as expressed in $\mathfrak{F}_p$. (Note in particular that $\hat{h}_{si}$ are the components of $\hat{\boldsymbol{h}}_s$ in the frame $\mathfrak{F}_c$, not in $\mathfrak{F}_p$.) What Roberson and Hooker found was that the relative equilibrium can be classified thus:

(i) General case:	$h_{s1}\neq 0$	$h_{s3}\neq 0$
(i) Conical case:	$h_{s1}=0$	$h_{s3}\neq 0$
(iii) Hyperbolic case:	$h_{s1}\neq 0$	$h_{s3}=0$
(iv) Cylindrical case:	$h_{s1}=0$	$h_{s3}=0$

(5)

The reason for the geometrical appelations can be understood from Fig. 2, which extends the helpful nomenclature and visualizations introduced by Likins[2] (in connection with the relative equilibria of spinning, symmetrical, rigid satellites) to the present more general case in which the rigid satellite is neither symmetrical nor spinning, but contains a rigid wheel that is symmetrical and spinning. To make this extension in nomenclature, one must select the wheel axis as the line that traces out a ruled surface as the gyrostat orbits Earth. (The present author has also shown that, in the "general" case, the surface generated by the wheel axis is in fact an *offset* hyperbola.)

It is evident both from Eq. (5) and from Fig. 2 that the conical and hyperbolic cases are degeneracies of the general case, and that the cylindrical case is, in turn, a further degeneracy of both the conical and hyperbolic cases. Reference 3 presents some figures that are very informative concerning the general case.

Brief Critique of Assumptions

The discussion thus far has been quite idealistic inasmuch as Earth's gravity is not exactly inverse-square, orbits can never be quite circular, and torques of other than gravitational origin are impressed on all space vehicles. Furthermore, the assumption of rigidity is well known to be inappropriate under certain circumstances. For this paper to be relevant to real spacecraft, further discussion is necessary.

The inverse-square assumption is a defensible simplification: Although higher harmonics in the gravity field can be significant for long-term orbit evolution, they are not relevant to the short-term attitude stability questions at issue here. With respect to the assumption of orbit circularity, we make the distinction between orbits that are intended to be circular (and that are in fact essentially circular) and orbits that are designed, for whatever reason, to be elliptical. The present analysis does not apply to the latter. As to the former, modern guidance and stationkeeping techniques can establish and

Received Jan. 20, 1984; revision received Oct. 15, 1984.

*Professor, Institute for Aerospace Studies. Associate Fellow AIAA.

maintain an orbit that is so nearly circular that circularity becomes a very strong assumption.

This brings us to two assumptions that are more troublesome. First, the role of gravitational torque. One can argue that this torque is, in a sense, more fundamental to a satellite than any other (no gravity, no orbit). At the same time, gravity torque is not dominant for all configurations at all altitudes. Indeed, it is quite common to have configurational symmetry such that, in the ideal orientation, gravity torque vanishes even while other environmental torques do not. Nevertheless, the conclusions of this paper will be applicable to situations where gravity is a major source of torque. For particular missions, detailed numerical simulations must always be resorted to for accuracy, while understanding must be provided by known analytical trends. This paper presents analytical trends.

Finally, we reflect on the assumption of rigidity. Let us first consider "passive" stabilization, i.e., the intrinsic, open-loop dynamics. If $\mathcal{W}$ is a momentum wheel, as in a bias-momentum satellite, rigidity for $\mathcal{W}$ is an excellent assumption. For an Earth-pointing dual-spin satellite, however, the rotor $\mathcal{W}$ may contain (among other things) sloshing fuel; as for $\mathcal{R}$, although the main body or platform can never be completely rigid, the "spin" of $\mathcal{R}$ (an absolute rotational rate of one revolution per orbital period) is very slow, so that the effects of energy dissipation in $\mathcal{R}$ will take a very long time to become manifest. Moreover, one can still assume for some decades to come that the first natural period of structural vibration of the platform is very short compared to the orbital period; therefore, as far as dynamical phenomena at orbital frequency are concerned (the subject of this paper) the satellite is essentially rigid.

Which brings us finally to interactions with an onboard "active" control system. The characteristic time for control system actions has in the past typically been shorter than the orbital period, but longer than a vehicle vibration period. This fact still makes justifiable the rigidity assumption for $\mathcal{R}$, although the control system is ignored in our analysis. For high-bandwidth controllers, the rigidity assumption is simply not tenable. Therefore the stability results in this paper may not be indicative of *closed-loop* behavior for actively controlled spacecraft, especially if they are quite flexible. The results are helpful, however, as regards *open-loop* behavior. In other words, they help to characterize the "plant" that the control system seeks to control. In this connection, we observe that the "rigid-body poles at the origin" are not, in fact, exactly at the origin; they may be (under conditions to be determined below) slightly in the right half plane, and thus open-loop unstable. It is precisely the identification of such dynamical instabilities to which this paper is addressed.

As a final remark on the "open-loop assumptions," spacecraft control systems occasionally do fail. Such failures can be expected at end-of-life, and earlier failures can and do occur. Open-loop dynamical behavior becomes very relevant after control system failures.

The Yaw-Wheel Class of Conical Equilibria

With reference to Fig. 2, we now concentrate on "conical equilibria," i.e., equilibria in which the stored angular momentum $\boldsymbol{h}_s$ has no component along the roll axis. As shown in Fig. 3, the general case has the axis of $\mathcal{W}$ at an angle β to the principal axis $\underline{\boldsymbol{p}}_2$, which, in turn, is at an angle χ to the pitch axis $\boldsymbol{c}_2$. Under present assumptions a relative equilibrium will occur[1] if

$$\sin(\chi+\beta)=\kappa\,\sin 2\chi \tag{6}$$

with

$$\kappa=\frac{2(I_2-I_3)\omega_c}{h_s}\equiv\frac{2}{\hat{h}_s}\left[1-\frac{I_3}{I_2}\right] \tag{7}$$

where $\hat{h}_s$ is the magnitude of $\hat{\boldsymbol{h}}_s$ and (I_1,I_2,I_3) are the principal inertias of $\mathcal{R}+\mathcal{W}$. A *relative* equilibrium is a state in which the relevant kinematical variables remain fixed (in the present instance, the orientation of $\mathcal{F}_p$ with respect to $\mathcal{F}_c$). In other words, the gyrostat attitude is fixed in the orbiting frame. Note that this state does not, however, imply a state of *dynamical* equilibrium, since a constant gravity-gradient roll torque impinges on the gyrostat. In fact, this gravitational torque is needed to precess the yaw component of stored angular momentum, $h_s\sin(\chi+\beta)$, once per orbit in order to sustain the equilibrium.

At this point, we introduce the inertia ratios

$$k_1\triangleq\frac{I_2-I_3}{I_1}\qquad k_3\triangleq\frac{I_2-I_1}{I_3} \tag{8}$$

as the significant dimensionless inertia parameters, in terms of which Eq. (7) becomes

$$\kappa=\frac{2k_1}{\hat{h}_s}\left[\frac{1-k_3}{1-k_1k_3}\right] \tag{9}$$

Two Important Subcases

Two important subcases of the conical equilibrium are now identified. The first is the "principal-axis-wheel" case for which $\beta=0$. The condition (6) reduces to

$$\cos\chi=(2\kappa)^{-1} \tag{10}$$

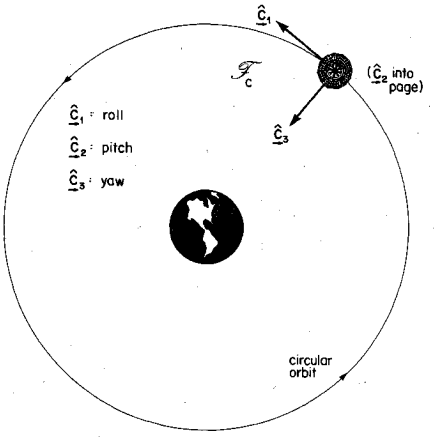

Fig. 1 Orbiting reference frame.

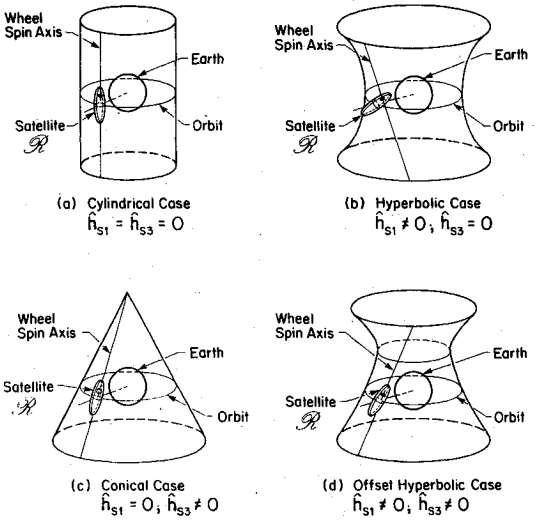

Fig. 2 Classification of relative equilibria for orbiting gyrostats.

after elimination of the cylindrical degeneracy. Stability for this case of equilibrium has been studied by Longman et al.[4]

Interest centers here on a different subcase, one characterized by a yaw-axis wheel (Fig. 4). The immediate application is to satellites for which, to achieve mission objectives, the principal axes of inertia cannot be aligned with the roll-pitch-yaw axes. A steady gravity-gradient torque must exist about the roll axis, and this must somehow be countered. A straightforward and practical design[5] is to incorporate a yaw-axis wheel, as shown.

Stability results (see the Appendix) for this subcase of the conical equilibrium have been published recently[6] and are summarized briefly in Fig. 5. Each k_1-k_3 plot [see Eq. (8)] has the equilibrium roll angle χ specified. (For example, each communications satellite design exemplified by Fig. 4 would require a certain value of χ.) In place of Eq. (10) for the principal-axis-wheel case, we now have

$$\chi+\beta=\pi/2 \tag{11}$$

whence, from Eq. (6),

$$\kappa=(\sin 2\chi)^{-1} \tag{12}$$

and the corresponding yaw-wheel momentum is then implied by Eq. (9). The regions marked *U* in Fig. 8 are "unstable"; those marked *S* are dynamically stable and statically stable; and those designated *D* are statically unstable but nevertheless gyroscoically stabilized (although such gyroscopically stabilized regions might shrink were specific mechanisms for energy dissipation to be introduced). The *D* regions are generalizations of the DeBra-Delp region[7] for a rigid Earth-pointing satellite ($\mathcal{W}=0$), as occurs in the first diagram in Fig. 5.

According to Fig. 5, *S*-regions are rare. Although present for $\chi=0$ deg and 90 deg ($\chi=90$ deg is physically identical to $\chi=0$ deg but wih an exchange of labels for the 2 and 3 principal axes), *S*-regions tend not to be present unless $\chi=n\pi/2$, where n is an integer. One of the contributions of this paper is to generalize these results (Fig. 5) by adding the beneficial effects of a pitch wheel.

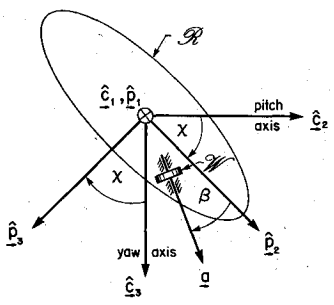

Fig. 3 Conical equilibrium: general case.

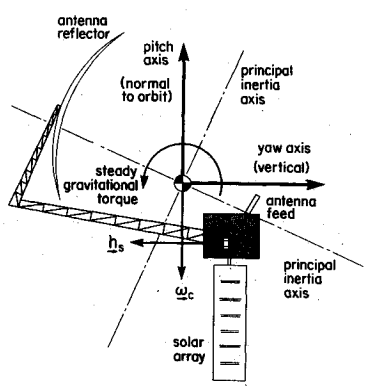

Fig. 4 Balance between steady gravity-gradient roll torque and steady reaction torque from yaw-axis wheel.

Pitch Wheel Added

The value of the component of stored angular momentum about the pitch axis is irrelevant to the existence and classification of equilibria, but this pitch component is highly relevant to the stability of those equilibria. It will in fact now be shown that a second wheel whose axis is aligned with the pitch axis represents an important design option in achieving stability. *Without* this pitch wheel, static stability of the conical equilibrium (yaw-axis wheel subcase) is unusual (Fig. 5). *With* the pitch wheel, many additional configurations can be stabilized.

The two-wheel situation (yaw wheel plus pitch wheel) is dynamically equivalent to that shown in Fig. 3. In the latter cas, let h_{s2} and h_{s3} represent the components in $\mathcal{F}_c$ of the stored angular momentum. Then the analogy is symbolized by the following equivalence:

$$\hat{h}_{s2}=\hat{h}_s\cos(\chi+\beta) \qquad \hat{h}_{s3}=\hat{h}_s\sin(\chi+\beta) \tag{13}$$

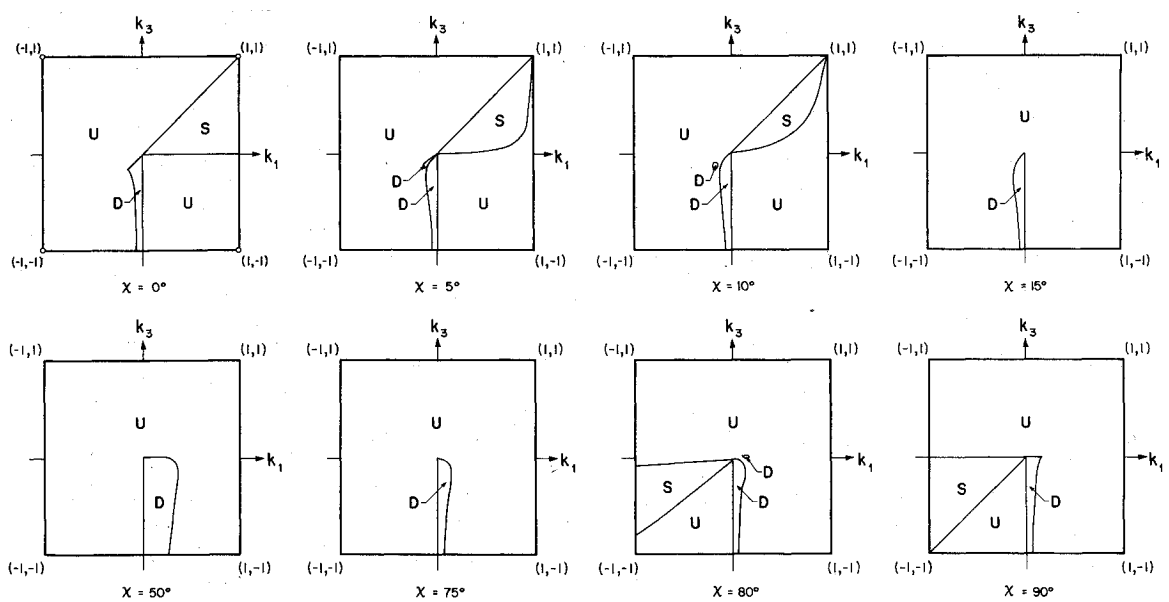

Fig. 5 Stability diagrams for orbiting gyrostat with yaw-axis wheel.

Thus, given a desired roll offset χ, one may pick either the pair $(\hat{h}_s, \beta)$ or the pair $(\hat{h}_{s2}, \hat{h}_{s3})$. It seems more likely that the latter option would be exercised in practice because, while β is impossible to alter in orbit, the speeds of two wheels could be commanded independently, thus making possible a wider range of possibilities.

Stability Results

The influence of the pitch-axis wheel is evident from Figs. 6-9. A glance at this series of figures shows the profound effect that pitch-wheel momentum can have on stability. (See the Appendix for algebraic details.) Thus, in Fig. 6, for $\chi = 10$ deg, it is clear that even a pitch-wheel momentum of $\hat{h}_{s2} = \pm 0.3$ can make a great difference from the no-pitch-wheel diagram shown for $\chi = 10$ deg in Fig. 5. As $|\hat{h}_{s2}|$ increases, first to 1.0 and then to 3.0, a pattern begins to emerge. The small region of static stability associated with no pitch wheel (Fig. 5) quickly disappears as $\hat{h}_{s2}$ becomes more positive; as $\hat{h}_{s2}$ continues to increase, however, an even larger region of gyroscopically stabilized cases develops until, for large positive $\hat{h}_{s2}$, much of the lower-right triangular half of the k_1-k_3 square consists of such cases. If, on the other hand, $\hat{h}_{s2}$ is increased negatively, the lower-right half of the first quadrant (corresponding to the condition $I_2 > I_1 > I_3$) is quickly stabilized, followed at $\hat{h}_{s2} = -1$ by the entire fourth quadrant ($I_1 > I_2 > I_3$). For even more negative values of $\hat{h}_{s2}$, portions of the third quadrant are also stabilized.

Largely similar remarks apply when the equilibrium roll angle χ is set at $\chi = 35$ deg, as evidenced by the diagrams in Fig. 7. For a roll offset of $\chi = 55$ deg, these trends continue, as shown in Fig. 8, although configurations in the upper left of the third quadrant are now gaining ascendancy over configurations in the lower right of the first quadrant. By the time χ reaches 80 deg (Fig. 9), it is clear that it is the lower half of the k_1-k_3 diagram that becomes stable as $|\hat{h}_{s2}|$ is increased; this stability is based on static stability for $\hat{h}_{s2} < 0$, and on gyroscopic stability for $\hat{h}_{s2} > 0$.

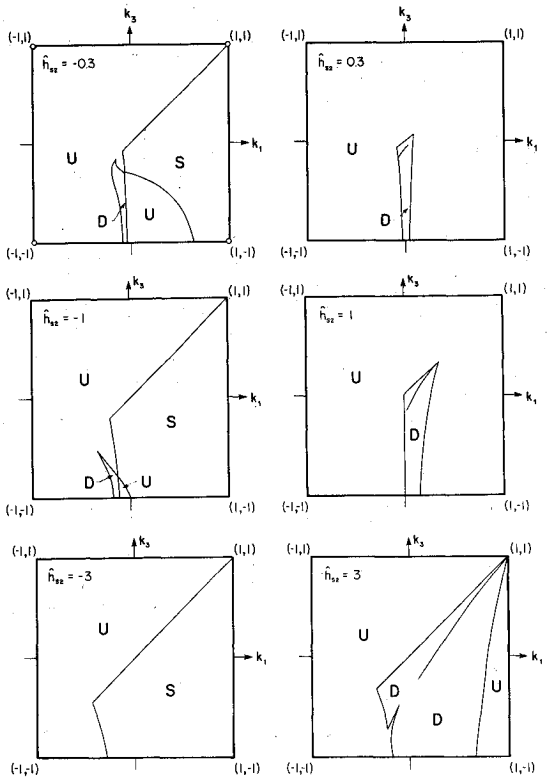

Fig. 6 Stability diagrams for orbiting gyrostat with yaw and pitch wheels ($\chi = 10$ deg).

Large Pitch-Wheel Momentum

It is likely that the application of these results will be to designs with relatively large values of pitch-wheel momentum:

$$|\hat{h}_{s2}| \gg 1 \tag{14a}$$

or, in dimensional terms,

$$|h_{s2}| \gg I_2 \omega_c \tag{14b}$$

In other words, the angular momentum of the pitch wheel will greatly exceed the pitch component of the (Earth-pointing) satellite's angular momentum that arises from its once-per-orbit rotation. This condition has certainly held true for all bias-momentum and dual-spin satellites to date, and it seems reasonable to apply a similar expectation to satellites of the type shown in Fig. 4. It also follows that we should assume

$$|\hat{h}_{s2}| \gg |\hat{h}_{s3}| \tag{15}$$

which is an assumption companion to Eq. (14). In rough physical terms, Eq. (15) requires that the pitch wheel be much larger than the yaw wheel.

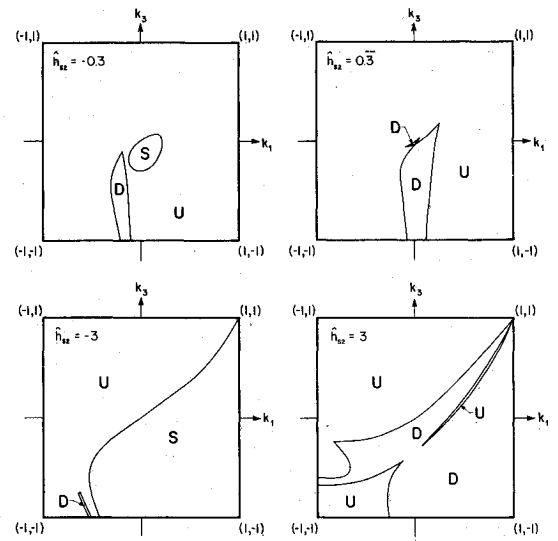

Fig. 7 Stability diagrams for orbiting gyrostat with yaw and pitch wheels ($\chi = 35$ deg).

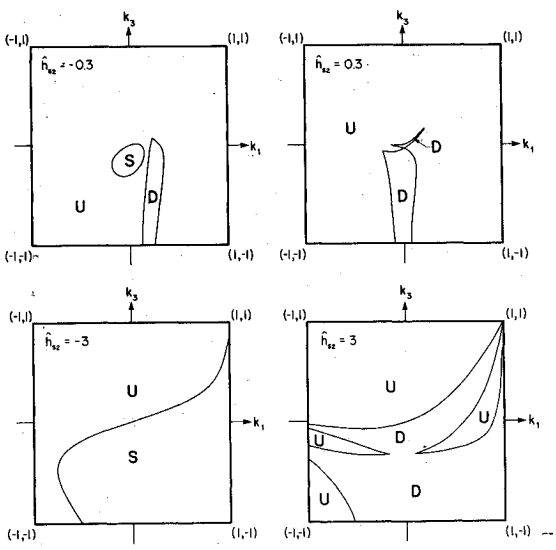

Fig. 8 Stability diagrams for orbiting gyrostat with yaw and pitch wheels ($\chi = 55$ deg).

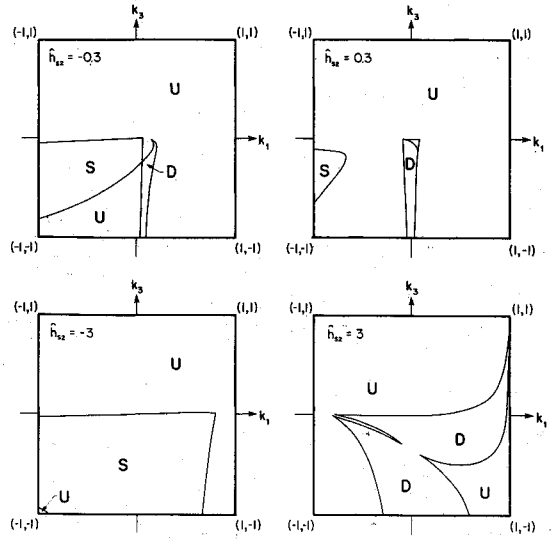

Fig. 9 Stability diagrams for orbiting gyrostat with yaw and pitch wheels ($\chi = 80$ deg).

The asymptotic form of the system characteristic equation, in the limiting case as $\hat{h}_{s2}$ becomes very large, is (see the Appendix)

$$a_0 s^6 + \hat{h}_{s2}^2 (a_1 s^2 + a_2)(s^2 + 1) = 0 \tag{16}$$

where

$$a_0 = I_1 I_1 I_3 \quad a_1 = I_2^2 \mathcal{I}_{22} \quad a_2 = 3I_2^2 (\mathcal{I}_{11} - \mathcal{I}_{33}) \tag{17}$$

and we recall that (I_1, I_2, I_3) are the principal inertias of the gyrostat in the body-fixed frame $\mathcal{F}_b$. The inertia matrix in the orbiting frame $\mathcal{F}_c$, on the other hand, is denoted $\mathcal{I}$. In fact,

$$\mathcal{I}_{11} = I_1 \quad \mathcal{I}_{22} = I_2 \cos^2\chi + I_3 \sin^2\chi \quad \mathcal{I}_{33} = I_2 \sin^2\chi + I_3 \cos^2\chi \tag{18}$$

It is evident from Eq. (16) that, as $|\hat{h}_{s2}| \to \infty$, two roots approach $\pm j$; the satellite attitude is fixed inertially in these two modes. Two more roots approach $\pm (a_2/a_1)^{1/2}$, and the last two approach $\pm j\infty$.

A rigorous stability analysis of Eq. (16), which for brevity we omit here, demonstrates that all conditions necessary and sufficient for stability are satisfied trivially, except $a_2 > 0$. Thus, from Eq. (17), we require that

$$\mathcal{I}_{11} - \mathcal{I}_{33} > 0 \tag{19}$$

which can be recognized as being similar to an elementary condition for gravity-gradient pitch stability. Roll and yaw stability, in turn, are taken care of by the pitch wheel. Furthermore, it can also be shown that this stability is "static" if $\hat{h}_{s2} < 0$ and "gyroscopic" if $\hat{h}_{s2} > 0$.

The form taken by Eq. (19) on a k_1-k_3 stability diagram is found by substitution of Eq. (18) and (8):

$$k_1 \cos^2\chi + k_1 k_3 \sin^2\chi - k_3 > 0 \tag{20}$$

In particular, if $\chi = 0$, we get $k_1 > k_3$, the basic gravity-gradient pitch stability condition (represented by the lower-right triangular half of the k_1-k_3 square); at the other extreme, we have $\chi = 90$ deg, in which case Eq. (20) reduces, since $k_1 < 1$, to $k_3 < 0$ (represented by the lower half of the k_2-k_3 square). For intermediate values of χ, the boundaries specified by Eq. (20) constitute a family of hyperbolas, one curve for each χ, passing through (1,1) and (0,0).

Hyperbolic Equilibria

It is also possible to define a family of "hyperbolic" equilibria (in the sense illustrated in Fig. 2) and to proceed along lines that are completely analogous to those used for the "conical" equilibria above. For hyperbolic cases, there is a steady-state *yaw* angle (in place of a steady-state *roll* angle). A roll-axis wheel is required to maintain equilibrium—not to counteract a gravitational torque (that torque is zero), but to make the total angular momentum vector of the satellite normal to the orbit (i.e., parallel to the pitch axis). The existence of such hyperbolic equilibria is not affected by an additional pitch-axis wheel, although stability characteristics can be greatly affected.

We shall not study the stability of the roll-axis-wheel class of hyperbolic equilibria in detail here, however, partly because the fundamental ideals are very similar to those just discussed and partly because applications for the hyperbolic equilibrium seem not to have emerged to parallel the conical equilibrium applications (for example, Fig. 4). The interested reader may wish to peruse Ref. 8, where many stability diagrams are recorded for both conical and hyperbolic equilibria.

Concluding Remarks

This paper contributes to the large body of literature on rigid gyrostats in orbit, and should also prove of practical interest in situations where gravitational torque dominates the attitude dynamics of a "conical-equilibrium" gyrostat. It suggests a new possibility for passive attitude stabilization—a conical equilibrium based on a yaw-axis wheel supplemented by a pitch-axis wheel. Moreover, in connection with active stabilization, the previous discussion serves to clarify the nature of the "plant" being controlled. This analysis should also prove predictively helpful for actively controlled conical-equilibrium gyrostats in the event of a control system failure.

Appendix: Stability Analysis

The variational equations for a conical-equilibrium gyrostat are

$$M\ddot{\alpha} + \omega_c G\dot{\alpha} + \omega_c^2 K\alpha = 0$$

with the coefficient matrices defined as follows:

$$M = \begin{bmatrix} \mathcal{I}_{11} & 0 & 0 \\ 0 & \mathcal{I}_{22} & \mathcal{I}_{23} \\ 0 & \mathcal{I}_{23} & \mathcal{I}_{33} \end{bmatrix}$$

$$G = \begin{bmatrix} 0 & -g_3 & g_2 \\ g_3 & 0 & 0 \\ -g_2 & 0 & 0 \end{bmatrix}$$

$$K = \begin{bmatrix} k_{11} & 0 & 0 \\ 0 & k_{22} & k_{23} \\ 0 & k_{23} & k_{33} \end{bmatrix}$$

The elements of these matrices are

$$\mathcal{I}_{11} = I_1 \qquad g_3 = -\tfrac{1}{2} I_2 \hat{h}_{33}$$

$$\mathcal{I}_{22} = I_2 \cos^2\chi + I_3 \sin^2\chi \qquad k_{11} = 4(\mathcal{I}_{22} - \mathcal{I}_{33}) - I_2 \hat{h}_{s2}$$

$$\mathcal{I}_{33} = I_2 \sin^2\chi + I_3 \cos^2\chi \qquad k_{22} = 3(\mathcal{I}_{11} - \mathcal{I}_{33})$$

$$\mathcal{I}_{23} = (I_2 - I_3)\sin\chi\cos\chi \qquad k_{33} = (\mathcal{I}_{22} - \mathcal{I}_{11}) - I_2 \hat{h}_{s2}$$

$$g_2 = (\mathcal{I}_{22} - \mathcal{I}_{11} - \mathcal{I}_{33}) - I_2 \hat{h}_{s2} \qquad k_{23} = \tfrac{3}{4} I_2 \hat{h}_{s3}$$

The characteristic equation is

$$\det[s^2M+s\omega_c G+\omega_c^2 K]=0$$

from which the location of the roots in the complex plane can be determined (the numerical method actually used to find eigenvalues may, however, be different, though equivalent, to finding the roots of the characteristic equation).

On the other hand, static stability corresponds to the condition $K>0$ for which necessary and sufficient conditions are

$$k_{11}>0 \qquad k_{22}>0 \qquad k_{22}k_{33}-k_{23}^2>0$$

Static stability is sufficient, but not necessary, for stability. Thus, we can distinguish between three possibilities, as indicated in the stability diagrams presented in the main text:

1) *U*—unstable; must have $Re\{s_\alpha\}>0$ for at least one root of the characteristic equation.

2) *S*—statically (and therefore dynamically) stable; must have $K>0$.

3) *D*—statically unstable but gyroscopically stabilized. $K\not>0$, but $Re\{s_\alpha\}=0$ for all roots of the characteristic equation.

Acknowledgments

This work was supported by a grant from the Natural Sciences and Engineering Research Council of Canada. The computer calculations were carried out by David Golla and the figures were prepared by Ida Krauze.

References

[1]Roberson, R.E. and Hooker, W.W., "Gravitational Equilibria of a Rigid Body Containing Symmetric Rotors," *Proceedings of the 17th Congress of the International Astronautics Federation,* Madrid, 1966.

[2]Likins, P.W., "Stability of a Symmetrical Satellite in Attitudes Fixed in an Orbiting Reference Frame," *Journal of the Astronautical Sciences,* Vol. No. 1, 1965, pp. 18-24.

[3]Longman, R.W. and Roberson, R.E., "General Solution for the Equilibria of Orbiting Gyrostats Subject to Gravitational Torques," *Journal of the Astronautical Sciences,* Vol. 16, March-April 1969, pp. 49-58.

[4]Longman, R., Hagedorn, P., and Beck, A., "Stabilization Due to Gyroscopic Coupling in Dual-Spin Satellites Subject to Gravitational Torques," *Celestial Mechanics,* Vol. 25, 1981, pp. 353-373.

[5]Staley, D.A., "Spacecraft Attitude Stabilization Methods—Final Report," ANCON Space Technology Corp., Rept. R. 803, April 1981.

[6]Hughes, P.C., "Attitude Stability for the Yaw-Wheel Class of Orbiting Gyrostats," *CASI Journal,* Vol. 29, Sept. 1983, pp. 268-284.

[7]DeBra, D.B. and Delp, R.H., "Rigid Body Attitue Stability and Natural Frequencies in a Circular Orbit," *Journal of the Astronautical Sciences,* Vol. 8, 1961, pp. 14-17.

[8]Hughes, P.C. and Golla, D.F., "Stability Diagrams for a Rigid Gyrostat in a Circular Orbit," University of Toronto Institute for Aerospace Studies Tech. Note 243, Jan. 1984.